33RD CONGRESS
OF THE INTERNATIONAL COUNCIL
OF THE AERONAUTICAL SCIENCES
STOCKHOLM, SWEDEN, 4-9 SEPTEMBER, 2022

ICAS 2022 SWEDEN

TRIBOLOGICAL AND STRUCTURAL EVALUATION OF 3D PRINTED EPOXY RESINS

George Catalin Cristea[1], Adriana Stefan[1], Krzysztof Krawczyk[2], Cristina Elisabeta Pelin[1]

& Sorina Ilina[1]

[1]INCAS – National Institute for Aerospace Research "Elie Carafoli", B-dul Iuliu Maniu 220, Bucharest 061126, Romania
[2]Joanneum Research Forschungsgesellschaft m.b.H., Leonhardstrasse 59, A-8010 Graz, Austria

Abstract

This paper aims to investigate the morpho structural behavior of 3D printed epoxy resin influenced by printing parameters and the periodic geometries of reactive materials, after the preliminary characterization of mechanical properties. The test specimens in this paper were made using reactive inkjet prototyping technology and compared to cast materials. The samples subjected to tribological tests were prototyped using different amounts of base and hardener (B/H ratio) and different patterns of printing the hardener. A batch of 9 samples with different periodic geometries was analyzed, evaluating the behavior of the material from a structural point of view.

Keywords: 3D printed polymers, dry sliding, SEM, friction coefficient

1. Introduction

Epoxy resins are widely used due to their excellent properties, especially in applications where thermal and chemical stability are required as well as mechanical properties. However, their use is limited by traditional mold making techniques as well as their high fragility. Three-dimensional printing is a technology that is expanding more and more, due to its versatility and ability to produce complex macroscopic structures with controllable properties at microscopic level [1].

Thus, in the last decade, additive manufacturing techniques by 3D printing have attracted much interest from academia and industry. Four main classes of 3D printing technologies can be identified, which construct objects by adding layer-by-layer material [2]: Stereolithography (SLA), Fused filament fabrication (FFF) or Fused Deposition Modelling (FDM), Selective Laser Sintering (SLS), Direct Ink Writing (DIW). Especially by direct ink writing, composites with complicated architectures can be printed using high viscosity materials eliminating the need to use a mold or other type of template [3].

Problems in selecting the appropriate materials for mechanical engineering components are one reason for the investigation of tribological properties of polymers, which has a duty to support industry. Considerable fundamental and practical information on polymer tribology has been published by Bowden and Tabor [4], Lee [5], Deleanu [6], Santner and Czichos [7], Botan [8], Briscoe [9], Picu [10] and Dowson [11].

The test specimens in this paper were made using reactive inkjet prototyping technology, a technique that allows the additive manufacturing of new composites based on thermosetting resins of epoxy-polyamine type and compared to cast materials. This technology allows both the printing of complex parts, without the need to cast or process them, but also the control of the microstructure. The materials developed were heterogeneous epoxy resins without additives, composed of hard and soft microscale subdomains, with contrast and spatial distribution and were designed by modelling so as to increase the total strength of the material, without compromising its strength and modulus.

This paper aims to investigate the morpho structural behavior influenced by printing parameters and the periodic geometries of reactive materials, after the preliminary characterization of mechanical properties. The changes that occurred during the tests performed in order to establish the optimization procedures, are analyzed by scanning electron microscopy.

2. Materials and methodology

2.1 Materials

The 2 components of the epoxy resin, Epinal IR77.49-A1 (base) and Epinal IH77.49-B2 (hardener) were provided by BTO Epoxy Ges. M.b.H.

2.2 3D printing technique

For the reactive printing of epoxy thermosets, it was used a custom modified Pixdro LP50 printing platform, equipped with a double printhead assembly manufactured by Suess Microtec (Figure 1A). The Printhead can be equipped with two Spectra S-series printheads with 128 nozzles each (Figure 1B). Typically, a SL printhead (nominal droplet volume = 80 pL) was used for the Resin and an SM printhead (50 pL) for the Hardner. Such choice of printheads allows, after optimizing the respective waveforms, to obtain a mixing ratio of R:H = 2:1 (w/w) at the same printing resolution (dpi). Such mixing ratio was shown to produce homogenous samples with mechanical properties comparable to casted samples. The optimal interval between reactive layers (Δt) was found to be 8 min. Due to the requirement of reactive printing to print serially with two print heads in one pass to allow in situ mixing (substrate coalescence), a dedicated software had to be developed. The new printing software allows the definition of a stack by applying the base material followed by multiple applications of the hardener and vice versa. This stack can be repeated as often as required and layer mirroring is also possible (e.g., Base-Hardener/Hardener-Base). Furthermore, depending on the number of stacks, the print heads are automatically raised to avoid collision with the cured layers.

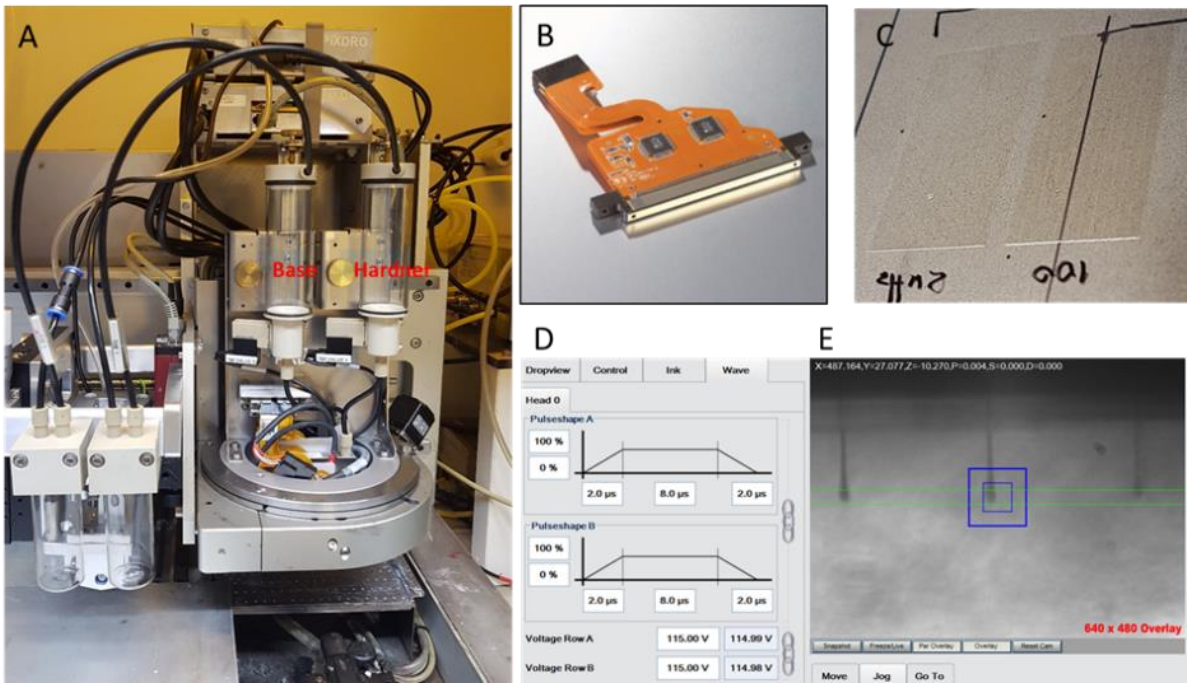

Figure 1 – Reactive printing of epoxy thermosets: (A) the double printhead assembly on a Pixdro LP50 printing platform; (B) a Spectra SL printhead with 128 piezoelectric nozzles; (C) layers of Resin and Hardener printed at various firing frequencies; (D) exemplary waveform optimized for the epoxy resin ink [R]; (E) droplets of ink [R] being fired from the printhead recorded in drop view position

Due to the process, there must be a printing pause between the stacks to give the hardener time to diffuse and thus cure/ gel the layer. However, in reactive printing in particular, an interruption in the printing process can lead to problems such as dewetting, nozzle clogging and even curing of the material in the print head. These problems are particularly pronounced for inks with short decap time; i.e., the time that inkjet nozzles can be uncovered and idle before requiring wiping or purging. The decap time is very short in the case of epoxy hardeners, which cures with atmospheric CO_2. Thus, the software was designed to allow the protection of the print heads by means of a special routine. This routine essentially consists of controlled firing of the individual nozzles at a very low frequency. This frequency was selected in such a way that the above-mentioned damage and/or problems could

not occur while minimizing the emitted material (waste). To allow the highest possible flexibility in the mixing ratios, the software was developed to work with vector graphics. This made it possible to print any resolution combinations (mixing ratios) without changing the structure size or its shape.
The materials studied in this paper vary from each other by: method of obtaining, by Base/Hardner (B/H) ratio, by the number of layers and by the method of adding the hardener. Table 1 presents the differences in terms of obtaining method for each material.

Table 1 - Different characteristics of the studied materials

Material	Obtaining method	B/H ratio	Number of layers	Measured thickness [mm]	Printing Order
35b	Casted	2:1	-	0.56	-
36b	Casted	2.75:1	-	0.53	-
15d	Printed	2.75:1	3	0.12	B/H
18b	Printed	2.75:1	10	0.5	B/H
21b	Printed	2:1	10	0.49	B/H
22b	Printed	2:1	10	0.5	B/Hx3
23b	Printed	2:1	10	0.51	B/Hx5
24b	Printed	2:1	10	0.48	B/Hx7
25b	Printed	2:1	10	0.55	B/Hx9

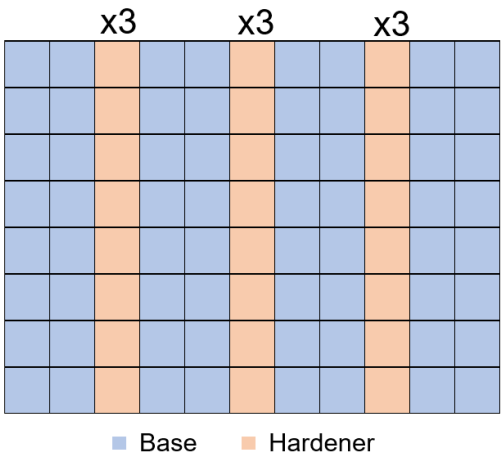

Figure 2 – Schematic example of 3D printed epoxy resin and hardener with a 3-layer hardener distribution “B/(Hx3)”

The printing of B and H was calibrated so that printing one layer with the same dpi (resolution) for B and H gives a weight ratio of B:H of 2:1 (2.75:1 for materials 36b, 15d and 18b). In this case, when printing a single layer of B and a single layer of H, the mix ratio is exactly 2:1. In order to obtain better printing and mixing results of the two components, H printing patterns were developed (Figure 2). This was added for every 3 layers (5, 7 or 9 layers). By doing so, the B/H ratio was no longer maintained and it was necessary to print the hardener several times on the same layer. In the case of B/Hx3 pattern, the printhead passed 3 times on layer 3, 6, 9 and so on. In the case of B/Hx5, the printhead passed 5 times on layer 5, 10 and so on. In this way the needed mixing ratio (2:1) was obtained.

2.3 Testing and analysis methodology

Roughness testing. In order to have a full evaluation of tribological behaviour, the specimens surface roughness was evaluated prior to tribological testing. The roughness was measured with C002 Insize surface roughness tester.

Tribological testing. The specimens obtained were subjected to tribological testing in order to evaluate the friction-wear behavior, and the changes that occurred following this test were analyzed by morphostructural characterization via scanning electron microscopy.

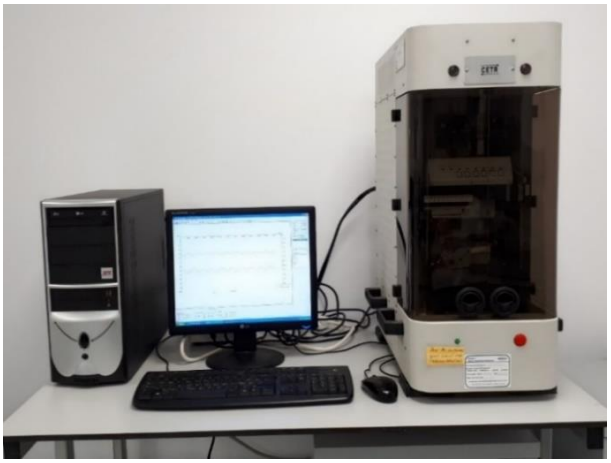

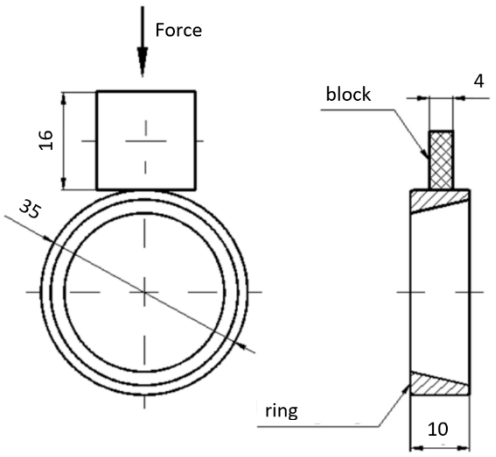

Figure 3 – Universal CETR UMT-3 Bruker equipment from INCAS (left); Schematic of block-on-ting test set-up (right)

Test specimens made of heterogeneous epoxy resins without additives, casted, or printed using reactive inkjet prototyping technology were tribologically tested using Universal CETR UMT-3 Bruker equipment from the Materials and Tribology Laboratory of the National Institute of Aerospace Research and Development "Elie Carafoli" - INCAS Bucharest (Figure 3). In order to evaluate the tribological behavior, dry tests were performed, using the block-on-ring module of the tribometer (Figure 3). The test process is described in ASTM G77-98 [12], specific to the above-mentioned procedure, which certifies the technique for determining wear after slip tests, for a range of materials, including polymeric materials. For testing according to the standard, the specimens shall measure 6.3 mm x 16 mm (± 0.2 mm); therefore, the materials were cut from larger specimens. For the ring, the outer casing of the radial-axial tapered roller bearing NTN A4138 was used, with an outer diameter of Ø34.988 mm and a width of 10.988 mm, and made of steel with a hardness of 60 - 62 HRC and a roughness Ra = 0.8 µm. For each test, a new pair of ring blocks was used. The tribological study was performed under the following conditions: sliding velocity - 100 rpm (0.183 m/s); normal force 10N, time - 10 min, temperature of the surrounding air 25 °C, relative humidity 60%. The testing procedure involved a preliminary stage of establishing the test parameters (force, speed, time), but also the method of attaching the materials to the surface of a metal block because they are in the form of films with very small thicknesses. Also, preliminary studies were performed to determine the minimum number of layers for which the tested materials do not break under the given test conditions.

Morpho-structural analysis. Morphostructural analysis was performed via scanning electron microscopy in order to evaluate the changes that occurred during the performed tribological tests, in order to establish the optimization procedures. Scanning electron microscopy was performed using SEM Quanta FEI 250 equipment at different magnification levels (x100-x150).

3. Results and discussion

Whereas for smooth surfaces and for polymer/polymer pairs in contact, adhesion may play a dominant role, the properties of a tribological system with a hard counter-body may be considerably influenced or changed by the surface roughness. This behavior has already been discussed in the literature in some detail [13-15] and it is shown for sample materials in Figure 4.

Table 2 shows the roughness of the samples measured with Insize surface roughness tester. The values presented represent the average of 3 measurements. The first column shows the roughness values measured on the print direction. The second column contains the roughness values in the direction perpendicular to the print line. Because the tribological tests were performed on the printing direction, only the roughness values in the first column were taken into account. The values of friction coefficients as a function of samples roughness are shown in the following figure.

Table 2 - The roughness of the tested materials

Material	**Roughness**, *Ra*		
	Along the printing direction	*Perpendicular to the printing direction*	
35b	0.015 µm		Casted samples
36b	0.013 µm		
15d	0.362 µm	0.781 µm	
18b	0.506 µm	0.894 µm	
21b	0.338 µm	0.803 µm	
22b	0.136 µm	0.689 µm	
23b	0.129 µm	0.492 µm	
24b	0.121 µm	0.965 µm	
25b	0.118 µm	0.457 µm	

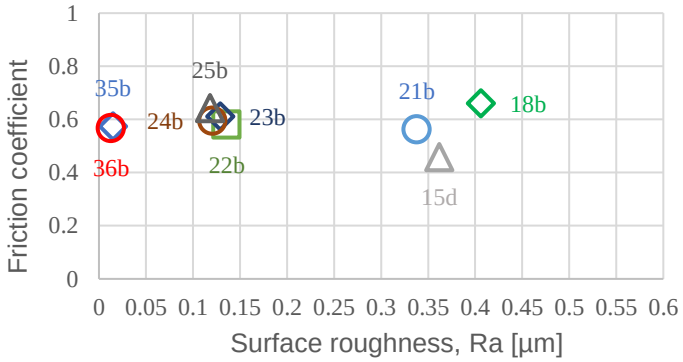

Figure 4 – Friction of polymer-steel pairs as a function of samples roughness

Analyzing Figure 4, the following aspects can be observed. The values of the coefficients of friction are not influenced in any way by the modification of the B/H ratio nor by the roughness of the surface of the specimen. These are in the range of 0.55-0.65, except for 15b specimen which has a coefficient of friction below 0.5. As expected, the roughness values for the cast specimens are small compared to the 3D printed ones, but an interesting aspect is given by the fact that the printed specimens with different hardening patterns (22b, 23b, 24b, 25b) have a roughness of 1.2 µm which is 3 times smaller than those on which the hardener was printed on each layer. All specimens deposited with hardener on each layer have roughness values of over 0.3 µm regardless of the number of printed layers.

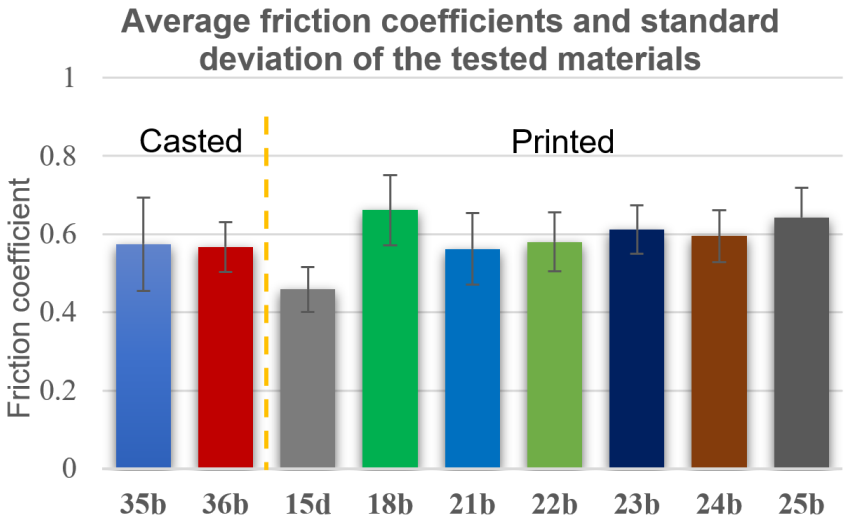

Figure 5 – Average friction coefficients and standard deviation of the tested materials

As previously presented, the average values of the coefficients of friction do not differ significantly regardless of the type of obtaining the specimens, and the standard deviations are within the limit of 20% compared to the average values. However, a slight increase can be observed with the distance of the hardener layers. The highest value of the coefficient of friction is given by test sample 18b. One explanation may be that a smaller amount of hardener was used.

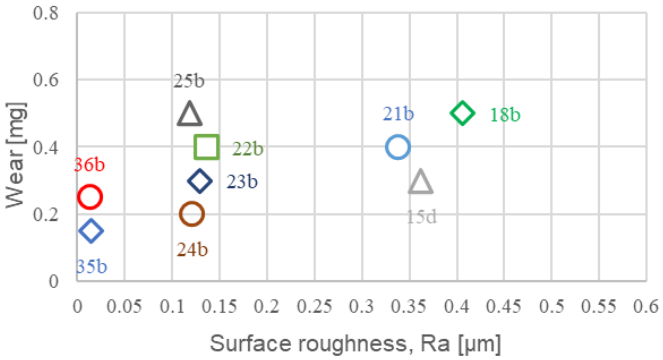

Figure 6 – Wear of polymers as a function of the roughness of the samples

Figure 6does not show a close correlation between the roughness of the specimens and their wear under the conditions presented. As expected, the lowest weight loss is attributed to the cast specimens. Quite close in value are specimens 24b, 15d and 23b. Surprisingly, the mass loss of specimen 24b (3d print) is less than the mass loss of specimen 36b (cast).

Morphological analysis was performed with the aid of scanning electron microscopy. The wear mechanism involved during tribological testing is important for the samples behavior evaluation and printed component-materials of the system response to the mechanical load. The micrographs were captured in the samples tested surface focused on the starting line and end line of testing.
Scanning electron microscopy was performed using SEM Quanta 250 equipment at different magnification levels (x100-x150).

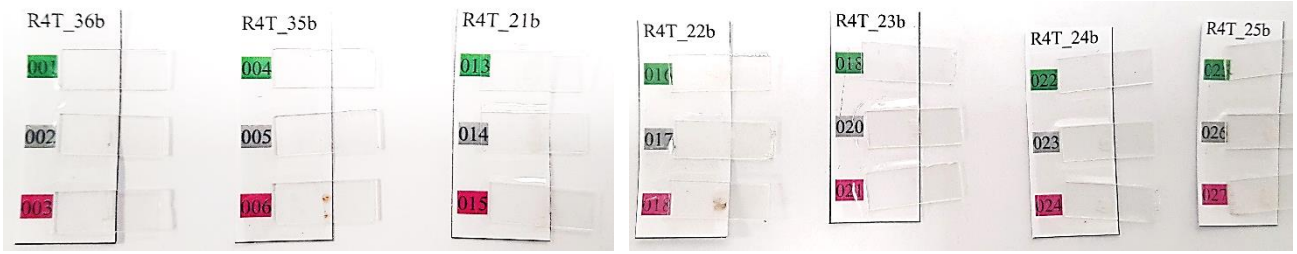

Figure 7 – Tribology specimens after testing and prepared for SEM analysis

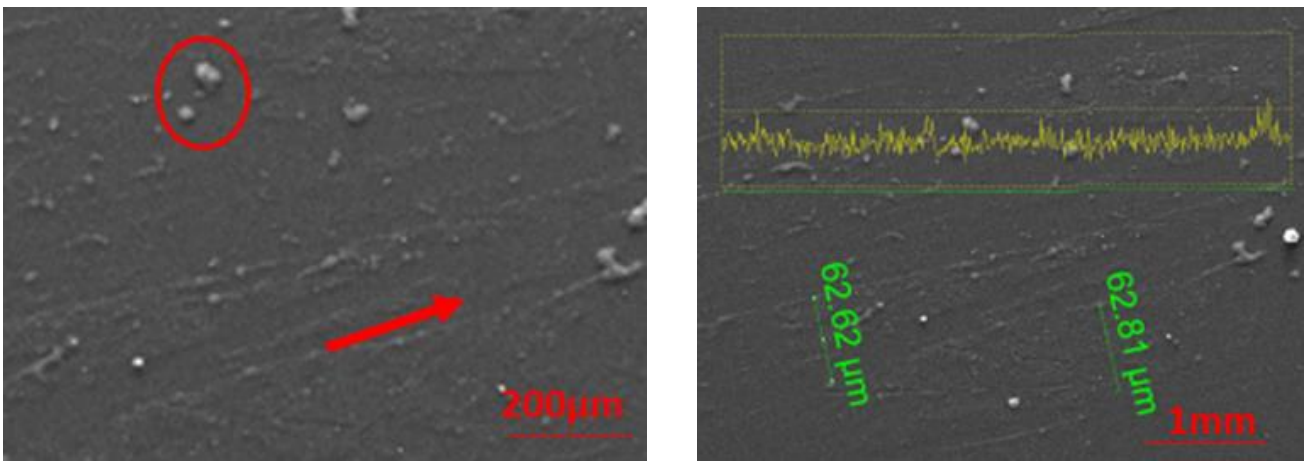

Figure 8 – SEM micrograph of control sample

The Figure 8 represents the control sample. The deposition cords with an average width of about 62 microns in the investigated area, are highlighted.

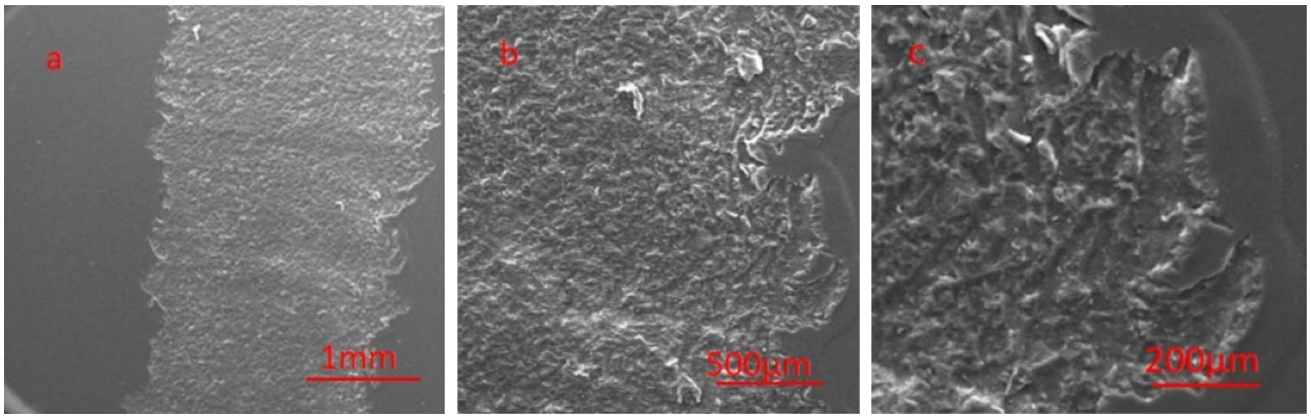

Figure 9 – Surface modification of the cast specimen 35b after tribology testing

Figure 9 illustrates the testing surface of the casted specimen 35b after testing. Figure 9a illustrates the entire area of testing, while Figure 9b, illustrates the details of tested area, in particular highlighting the end of the contact area. Figure 9c illustrates the morphological architecture of surface after testing, confirming that during the test, the tearing of the material occurred, with detached material parts in restricted area.

Figure 10 illustrates the testing surface of the casted specimen 36b after testing. Figure 10a illustrates the entire area of testing, while Figure 10b, illustrates the end of the contact area, where it can be observed that the morphology is specific to a polymer. Figure 10c illustrates the architecture of surface after testing confirming that during testing, the detachment of material occurred in the contact area, and the tearing of material occurred in restricted area.

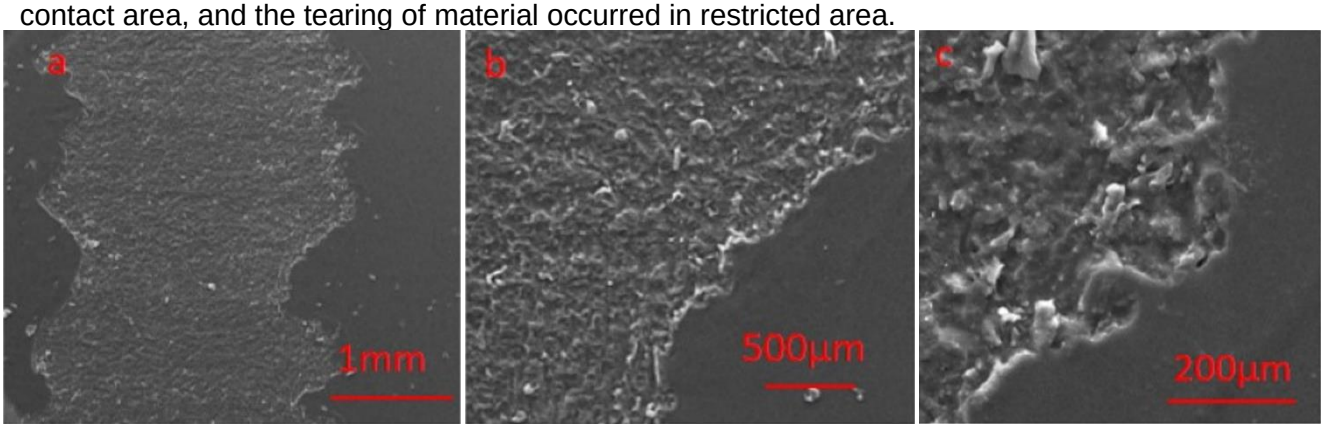

Figure 10 – Surface modification of the cast specimen 36b after tribology testing

The images of the tested samples are rendered in the contact areas of the material following the worn surfaces along the printing line.

Figure 11 illustrates the testing surface of the specimen 15d after testing. Figure 11a illustrates the entire area of testing, while Figure 11b, illustrates the dimension of tested area. Figure 10c illustrates the morphological architecture of surface after testing, confirming the materials tearing occurred during the test.

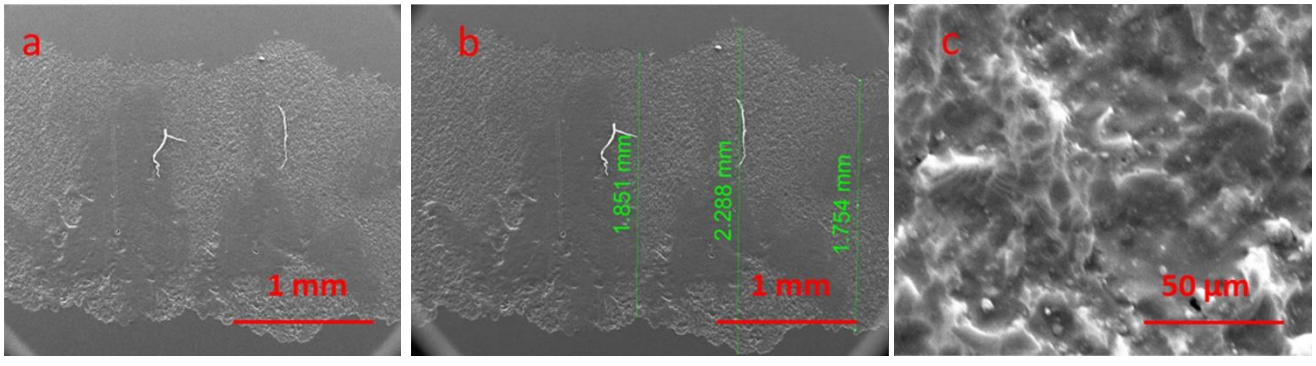

Figure 11 – SEM micrographs of sample 15d after tribological testing

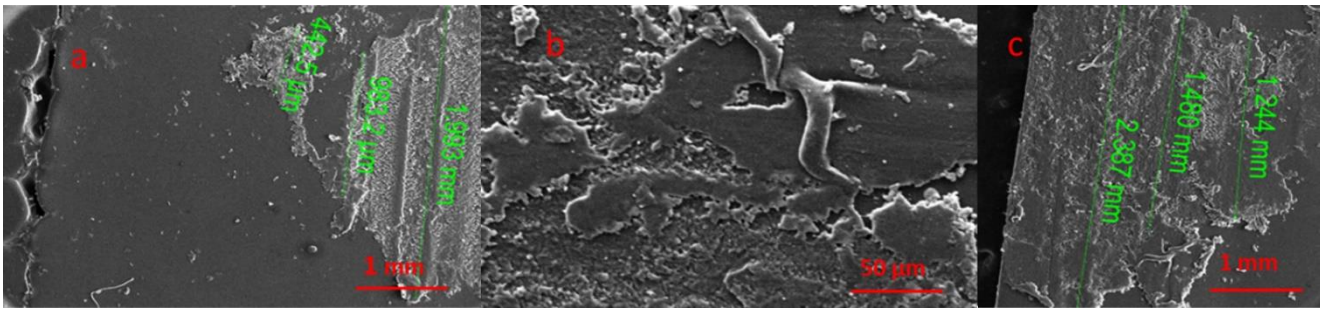

Figure 12 – SEM micrographs of sample 18b after tribological testing

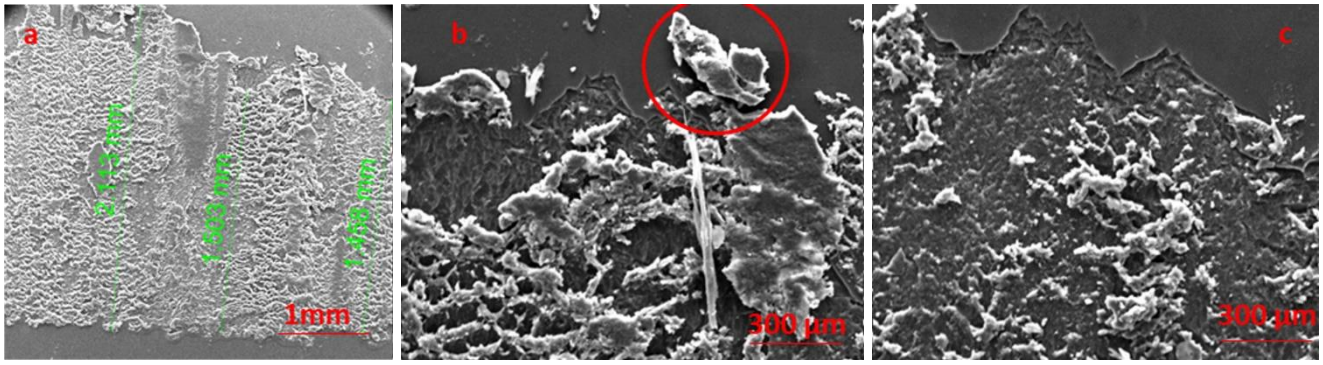

Figure 13 – SEM micrographs of sample 22b after tribological testing

The Figure 12 illustrates the testing surface of 18b specimen after testing. The Figure 12a illustrates the beginning of contact area, where the contact area is smooth without excess material, while the Figure 12c illustrate the ending of contact area where areas with materials detachment can be observed. Figure 12b illustrates surface with details from the detachment area.
The Figure 13 illustrates the testing surface of 22 b specimen after testing. The Figure 13a illustrates the entire area of contact with specific morphology for polymer, while Figure 13c illustrates the ending of contact area where areas with materials detachment can be observed and the ending line is clearly delimitated. Figure 13b illustrates surface with details from the detachment area in the sliding plane.

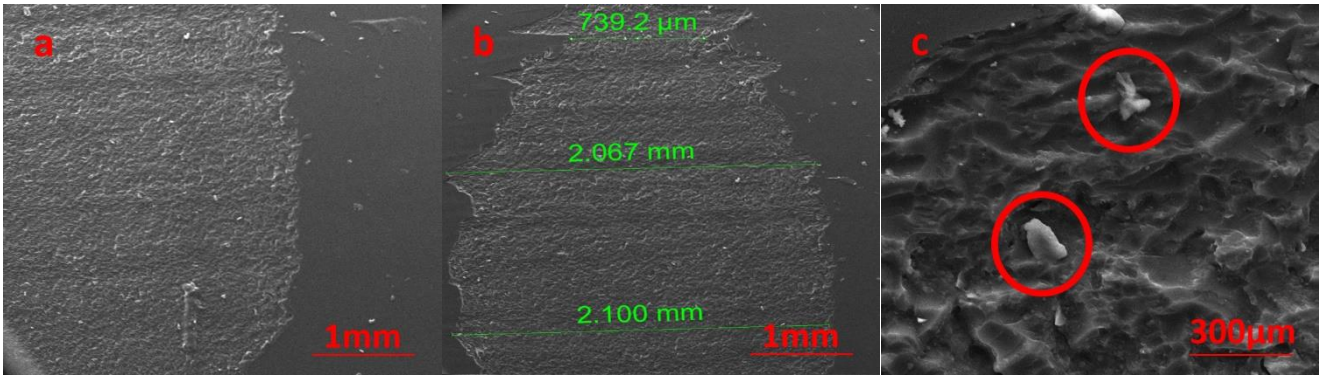

Figure 14 – SEM micrographs of sample 24b after tribological testing

Figure 14 illustrates the test surface of the 24b specimen after testing. Figure 14b illustrates the entire contact area with the specific morphology for the polymer [16-17], while Figure 14a shows the end of the contact area where the areas where the transfer of polymeric material took place can be seen with the material detachment and the end line which is clearly delimited. Figure 14c illustrates the surface with details of the transfer area having a specific morphology. The cylindrical shape of the crystalline structure of the polymer is highlighted, slightly modified in the adhesion process between the polymer and the metal, in the sliding plane. A few „lumps" of polymer are observed in restricted area.

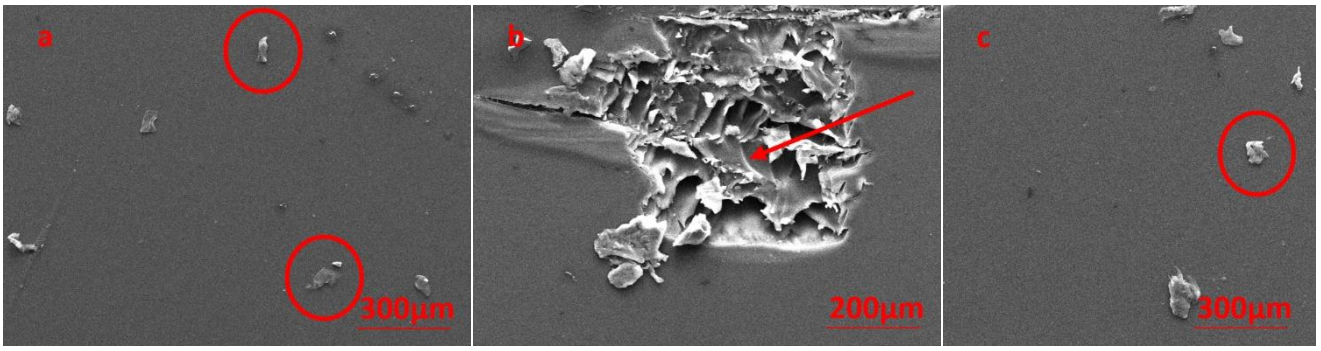

Figure 15 – SEM micrographs of sample 21b after tribological testing

Figure 15 illustrates the test surface of the 21b specimen after testing. Figure 15a illustrates the entire contact area with the specific uniform morphology of the polymer, while Figure 15b shows the lateral area of the contact area. The area where the transfer of polymeric material took place on the metal surface is highlighted and detachments of polymeric material can be seen in the adhesion area. Figure 15c illustrates the end of the contact area. It can be observed the morphology specific to the polymer, without material detachment in the contact area, but there are a few „lumps" of polymers on the investigated surface, most probably from the adhesion area.

Scanning electron microscopy analysis shows that the cast versus printed specimens behave similarly in terms of tribological testing response, while the number of layers for printed specimens do not influence the detachment behavior.

4. Conclusions

Analyzing both the coefficient of friction and the wear of the specimens, it can be concluded that the printing method that offers material solutions with a tribological behavior as close as possible to the behavior of cast materials are the patterns B/Hx5 and B/Hx7, where the hardener is deposited every 5 layers and respectively every 7 layers. In order to obtain lower roughness of the material, it is preferable for the hardener not to be printed on each layer.

Morphology images show that the transfer of polymeric materials took place in the contact area specially in the end line which is clearly delimited. The cylindrical shape of the crystalline structure of the polymer is highlighted in the image of 24b sample, slightly modified in the adhesion process between the polymer and the metal, in the sliding plane. In the both cases, cast and printed samples, a similarity of the detachment mechanism is observed in the contact area. The torn material parts can be seen in all cases.

The number of layers or concentration, does not influence the detachment mechanism of the materials during friction. The morpho structural architecture of the printed system is slightly modified during testing, without major influence in the wear process, probably due to the overheating in the contact area.

The study presents the tribological testing response of 3D printed versus cast epoxy resin materials, evaluating the specimens' roughness, friction coefficient and morphostructural modification generated by the friction testing. The results show that samples in which the hardener is deposited every 5 or 7 layers are the most similar to the cast ones, but overall, the tribological behavior does not illustrate major differences. These results are particularly useful for the applications range of the 3D printed epoxies in comparison to the cast manufactured ones, in order to have besides a full analogy development between the methods, also some indicatives of the materials' behavior depending on the obtaining route.

5. Contact Author Email Address

mailto: cristea.george@incas.ro

6. Copyright Statement

and distribution of this paper as part of the ICAS proceedings or as individual off-prints from the proceedings.

7. Acknowledgement

This work was supported by the project “Reactive Inkjet Printing of Epoxy Thermoset Composites” (RIPE4TEC), in the framework of Program 3- International and European Cooperation- Subpogram 3.2- Horizon 2020- M-ERA.Net Call 2019, funded by The Executive Unit for Financing Higher Education, Research, Development and Innovation ─ UEFISCDI Romania and by the European Union’s Horizon 2020 Research and Innovation Programme.

References

[1] Maguire A, Pottackal N, Saadi M. A. S. R, Rahman M. M, Ajayan P. M. Additive manufacturing of polymer-based structures by extrusion technologies. *Oxford Open Materials Science*, Vol. 1, 2020.

[2] Manning K. B, Wyatt N, Hughes L, Cook A, Giron N. H, Martinez E, Campbell C. G, Celina M. C. Self-assembly assisted additive manufacturing of an epoxy- amine resin. *Macromol. Mater. Eng.,* Vol. 304, No. 3, 2018.

[3] Tagliaferri S, Panagiotopoulos A, Mattevi C. Direct ink writing of energy materials. *Materials Advances,* Vol. 2, No. 2, pp 540-563, 2021.

[4] Bowden F. P, Tabor D. The friction and lubrication of solids, part II. *Clarendon Press: Oxford University Press,* Vol. 7, pp 557-558, 1964.

[5] Lee L. H. Advances in polymer friction and wear. *Polymer Science and Technology Series,* 1st edition, Springer New York, 1974.

[6] Deleanu L, Botan M, Georgescu C. Tribological behavior of polymers and polymer composites. *Tribology in Materials and Manufacturing-Wear, Friction and Lubrication,* IntechOpen: London, UK, 2020.

[7] Santner E, Czichos H. Tribology of polymers. *Tribology International,* Vol. 22, No. 2, pp. 103-109, 1989.

[8] Botan M, Roman I, Georgescu C, Cantaragiu A, Deleanu L. Tribological performance of the blend PBT and short aramid fibers. *INCAS Bulletin*, Vol. 7, No. 1, pp 29–36, 2015.

[9] Briscoe B. Wear of polymers: an essay on fundamental aspects. *Tribology International,* Vol. 14, No. 4 pp. 231-243, 1981.

[10] Picu C. R, Krawczyk K. K, Wang Z, Pishvazadeh-Moghaddam H, Sieberer M, Lassnig A, Kern W, Hadar A, Constantinescu D. M. Toughening in nanosilica-reinforced epoxy with tunable filler-matrix interface properties. *Composites Science and Technology*, Vol. 183, 2019.

[11] Dowson D, Godet M, Taylor C. M. Wear of non-metallic materials. *Mechanical Engineering Publications*, London 1978.

[12] ASTM G77-98, Standard test method for ranking resistance of materials to sliding wear.

[13] Uetz H, Breckel H. Friction and wear tests with PTFE. *Wear*, Vol. 10, pp. 185-198, 1967.

[14] Buckley D. H. Surface effects in adhesion, friction, wear and lubrication. *Elsevier*, New York, 1981.

[15] Lancaster J. K. Friction and wear. *Polymer science: A material science hand book*, Jenkins A.D. (ed), North Holland, Amsterdam, pp. 959-1046, 1972.

[16] Pelin C. E, Pelin G, Andronescu E, Ficai A, Ştefan A, Truşcă R, Vasile E. Effect of layered silicates on mechanical properties of carbon fiber fabric epoxy laminated composites. *U.P.B. Scientific Bulletin*, Series B, Vol. 78, No. 1, pp. 27-38, 2016.

[17] McCooka N. L, Burrisa D. L, Bournea G. R, Steffensa J, Hanrahanb J. R, Sawyera W. G. Wear resistant solid lubricant coating made from PTFE and epoxy. *Tribology Letters*, Vol. 18. No. 1, 2005.